IMPROVE

INTERAGENCY MONITORING OF PROTECTED VISUAL ENVIRONMENTS

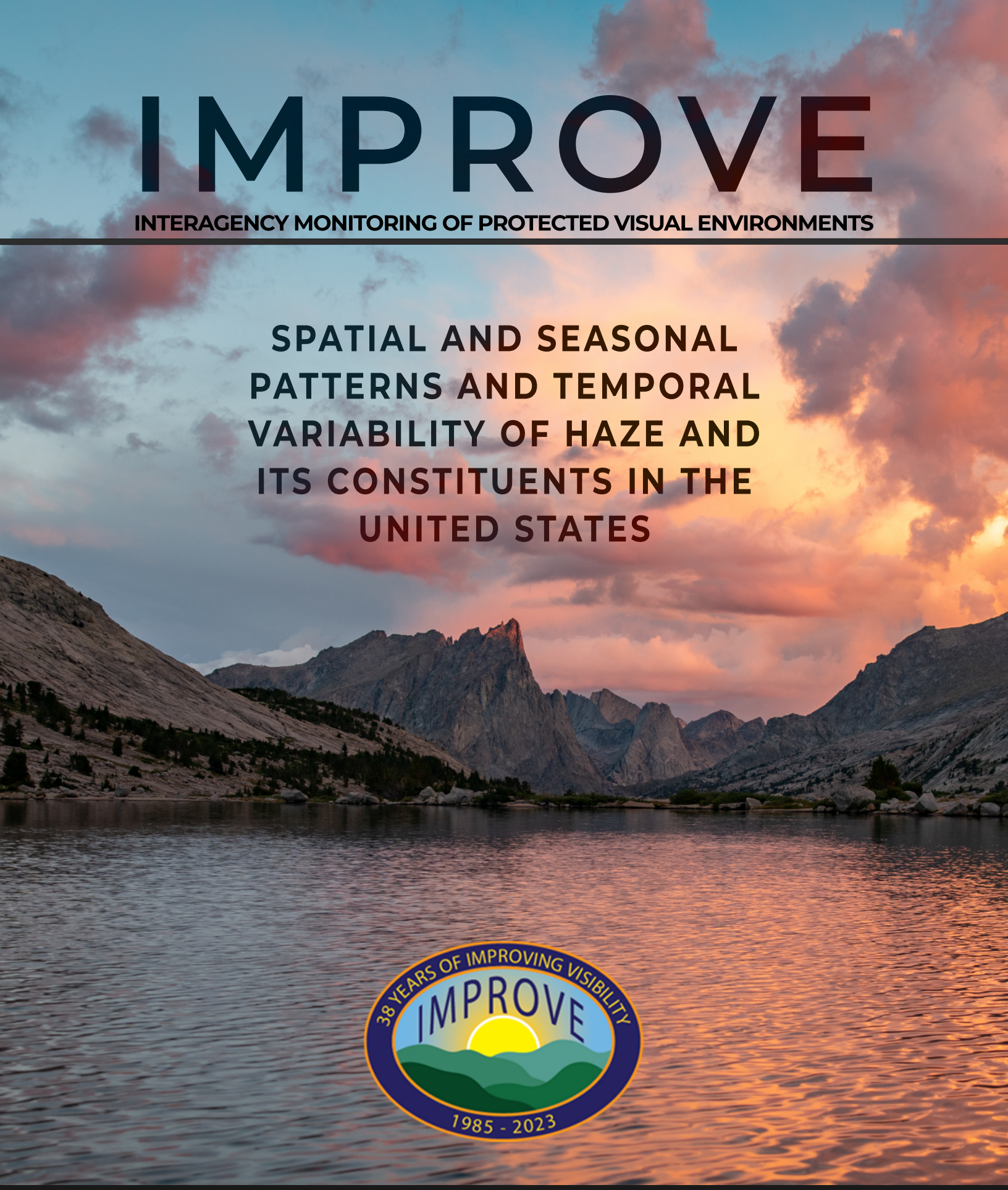

SPATIAL AND SEASONAL PATTERNS AND TEMPORAL VARIABILITY OF HAZE AND ITS CONSTITUENTS IN THE UNITED STATES

38 YEARS OF IMPROVING VISIBILITY
IMPROVE
1985 - 2023

COLORADO STATE UNIVERSITY

REPORT VI
2023

CIRA

We dedicate this report to all of the hard working operators, technicians, and scientists who have contributed to the success of the IMPROVE network over the years.

Description of the cover:
Deep Lake in the Bridger Wilderness, Wyoming (photo credit: Scott Copeland)

Spatial and Seasonal Patterns and Temporal Variability of Haze and its Constituents in the United States
Report VI

Principal Author:
Jenny L. Hand[1]

[1]Cooperative Institute for Research in the Atmosphere
Colorado State University
Fort Collins, CO 80523-1375

Contributors:

Scott A. Copeland[1]
Judy Chow[2]
Ann M. Dillner[3]
Nicole P. Hyslop[3]
William C. Malm[1]
Anthony J. Prenni[4]
Sean M. Raffuse[3]
Bret A. Schichtel[4]
John G. Watson[2]
Dominique E. Young[3]
Xiaolu Zhang[3]

[2]Desert Research Institute
Reno, NV 89512

[3]Air Quality Research Center
University of California
Davis, CA 95618

[4]National Park Service
Air Resources Division
Lakewood, CO 80225

Disclaimer
The assumptions, findings, conclusions, judgments, and views presented herein are those of the authors and should not be interpreted as necessarily representing the National Park Service or National Oceanic and Atmospheric Administration policies.

TABLE OF CONTENTS

Executive Summary S-1

S.1 Introduction S-1

S.2 Aerosol Data S-2

S.3 Spatial Patterns in Rural and Urban Speciated Annual Mean Aerosol Concentrations S-6

S.3.1 Ammonium Sulfate S-7

S.3.2 Ammonium Nitrate S-7

S.3.3 Particulate Organic Matter S-8

S.3.4 Elemental Carbon S-9

S.3.5 Fine Dust S-9

S.3.6 Sea Salt S-10

S.3.7 $PM_{2.5}$ Gravimetric Mass S-10

S.3.8 Coarse Mass S-11

S.3.9 Discussion S-11

S.4 Seasonal Distributions in Aerosol Mass Concentrations S-12

S.4.1 Ammonium Sulfate S-13

S.4.2 Ammonium Nitrate S-19

S.4.3 Particulate Organic Matter S-20

S.4.4 Elemental Carbon S-20

S.4.5 Fine Dust Mass S-21

S.4.6 $PM_{2.5}$ Sea Salt S-22

S.4.7 $PM_{2.5}$ Gravimetric Fine Mass S-22

S.4.8 Discussion S-23

S.5 Spatial and Seasonal Patterns in Relative Reconstructed Aerosol Light Extinction Coefficients S-25

S.5.1 Annual Mean Reconstructed Light Extinction Coefficient S-25

S.5.2 Ammonium Sulfate Light Extinction Coefficients S-27

S.5.3 Ammonium Nitrate Light Extinction Coefficients S-32

S.5.4 Particulate Organic Matter Light Extinction Coefficients S-33

S.5.5 Elemental Carbon Light Extinction Coefficients S-34

S.5.6 Fine Dust Light Extinction Coefficients S-34

S.5.7 $PM_{2.5}$ Sea Salt Light Extinction Coefficients S-35

S.5.8 Coarse Mass Light Extinction Coefficients S-35

S.5.9 Discussion S-36
S.6 Trends in IMPROVE Speciated Aerosol Mass Concentrations S-38
S.6.1 Sulfate Ion Trends S-39
S.6.2 Nitrate Ion Trends S-40
S.6.3 Organic Carbon Trends S-42
S.6.4 Elemental Carbon Trends S-43
S.6.5 Fine Dust Trends S-44
S.6.6 Gravimetric $PM_{2.5}$ Fine Mass Trends S-46
S.6.7 Coarse Mass Trends S-47
S.6.8 Discussion S-49
REFERENCES S-52
Chapter 1. Interagency Monitoring of Protected Visual Environments (IMPROVE) Network: Configuration and Measurements 1-1
1.1 Introduction 1-1
1.2 Overview of the Improve Monitoring Network 1-4
1.2.1 Site Locations 1-4
1.2.2 Aerosol Sampling and Analysis 1-15
1.2.3 Optical Monitoring and Analysis 1-24
1.3 Protocol and Equipment Changes 1-29
1.3.1 Analytical Changes 1-29
1.3.1.1 Carbon Analyzer Replacements 1-29
1.3.1.2 Environmentally Controlled Chamber Measurements of $PM_{2.5}$ and PM_{10} Gravimetric Mass 1-30
1.3.1.3 Transition from Custom-built XRF Instruments to PANalytical Epsilon 5 Instruments 1-31
1.3.1.4 Changes to Filter Light Absorption Measurement (f_{abs}) 1-33
1.3.1.5 Fourier Transform-Infrared Spectroscopy (FT-IR) 1-35
1.3.1.6 Summary of Data Advisories 1-36
1.3.1.7 Quality Assurance Reports 1-40
1.3.2 Sampling Equipment Changes 1-40
1.3.2.1 New Sampler Controller 1-40
1.3.2.2 Teflon Manufacture Change 1-40
1.3.3 Data Processing Changes 1-41
1.3.4 Summary of Changes 1-43
1.3.5 IMPROVE Technical System Audits 1-44

1.4 Chemical Speciation Network 1-45
REFERENCES 1-55
Chapter 2. Spatial Patterns of Speciated $PM_{2.5}$ Aerosol Mass Concentrations 2-1
2.1 Aerosol Species Composition 2-2
2.2 Spatial Patterns in Annual Mean Mass Concentrations 2-4
2.2.1 $PM_{2.5}$ Ammonium Sulfate Mass 2-4
2.2.2 $PM_{2.5}$ Ammonium Nitrate Mass 2-7
2.2.3 $PM_{2.5}$ Particulate Organic Matter Mass 2-10
2.2.4 $PM_{2.5}$ Elemental Carbon Mass 2-13
2.2.5 Filter Light Absorption (f_{abs}) 2-16
2.2.6 $PM_{2.5}$ Fine Dust Mass 2-17
2.2.7 $PM_{2.5}$ Sea Salt Mass 2-21
2.2.8 $PM_{2.5}$ Gravimetric Fine Mass 2-24
2.2.9 $PM_{2.5}$ Reconstructed Fine Mass 2-26
2.2.10 $PM_{2.5}$ Residual 2-27
2.2.11 PM_{10} Mass 2-29
2.2.12 Coarse Mass 2-30
2.2.13 Summary 2-33
REFERENCES 2-36
Chapter 3. Seasonal Distributions of $PM_{2.5}$ Aerosol Mass 3-1
3.1 $PM_{2.5}$ Ammonium Sulfate 3-2
3.1.1 IMPROVE 3-2
3.1.2 CSN 3-8
3.2 $PM_{2.5}$ Ammonium Nitrate 3-14
3.2.1 IMPROVE 3-14
3.2.2 CSN 3-15
3.3 $PM_{2.5}$ Particulate Organic Matter 3-16
3.3.1 IMPROVE 3-16
3.3.2 CSN 3-17
3.4 $PM_{2.5}$ Elemental Carbon 3-18
3.4.1 IMPROVE 3-18
3.4.2 CSN 3-19
3.5 $PM_{2.5}$ Dust Mass 3-19
3.5.1 IMPROVE 3-19

3.5.2 CSN 3-20
3.6 $PM_{2.5}$ Sea Salt Mass 3-21
3.6.1 IMPROVE 3-21
3.6.2 CSN 3-22
3.7 $PM_{2.5}$ Gravimetric Fine Mass 3-23
3.7.1 IMPROVE 3-23
3.7.2 CSN 3-23
3.8 Coarse Mass 3-23
3.9 Discussion 3-27
REFERENCES 3-30
Chapter 4. Reconstructed Aerosol Light Extinction Coefficients 4-1
4.1 IMPROVE Aerosol Light Extinction Coefficient Algorithm 4-1
4.2 Spatial Patterns in Annual Mean Aerosol Light Extinction Coefficients 4-5
4.2.1 $PM_{2.5}$ Ammonium Sulfate Light Extinction Coefficients 4-5
4.2.2 $PM_{2.5}$ Ammonium Nitrate Light Extinction Coefficients 4-8
4.2.3 $PM_{2.5}$ Particulate Organic Matter Light Extinction Coefficients 4-11
4.2.4 $PM_{2.5}$ Elemental Carbon Light Extinction Coefficients 4-14
4.2.5 $PM_{2.5}$ Fine Dust Light Extinction Coefficients 4-17
4.2.6 $PM_{2.5}$ Sea Salt Extinction Coefficients 4-20
4.2.7 Coarse Mass Light Extinction Coefficients 4-22
4.2.8 Reconstructed Aerosol Light Extinction Coefficients 4-25
4.2.9 Reconstructed Total Light Extinction Coefficients 4-27
4.2.10 Deciview 4-28
4.2.11 Summary 4-29
REFERENCES 4-32
Chapter 5. Seasonal Distribution of Reconstructed Aerosol Light Extinction Coefficients . 5-1
5.1 $PM_{2.5}$ Ammonium Sulfate Light Extinction Coefficients 5-1
5.1.1 IMPROVE 5-1
5.1.2 CSN 5-8
5.2 $PM_{2.5}$ Ammonium Nitrate Light Extinction Coefficients 5-14
5.2.1 IMPROVE 5-14
5.2.2 CSN 5-16
5.3 $PM_{2.5}$ Particulate Organic Matter Light Extinction Coefficients 5-17
5.3.1 IMPROVE 5-17

5.3.2 CSN 5-19
5.4 $PM_{2.5}$ Elemental Carbon Light Extinction Coefficient 5-20
5.4.1 IMPROVE 5-20
5.4.2 CSN 5-21
5.5 $PM_{2.5}$ Fine Dust Light Extinction Coefficients 5-22
5.5.1 IMPROVE 5-22
5.5.2 CSN 5-23
5.6 $PM_{2.5}$ Sea Salt Light Extinction Coefficients 5-24
5.6.1 IMPROVE 5-25
5.6.2 CSN 5-26
5.7 Coarse Mass Light Extinction Coefficients 5-26
5.7.1 IMPROVE 5-26
5.7.2 CSN 5-28
5.8 Reconstructed Aerosol Light Extinction Coefficients 5-29
5.8.1 IMPROVE 5-29
5.8.2 CSN 5-30
5.9 Deciview 5-31
5.9.1 IMPROVE 5-31
5.9.2 CSN 5-31
5.10 Summary 5-32
Chapter 6. Trends in IMPROVE Speciated Aerosol Concentrations 6-1
6.1 Sulfate Ion Trends 6-2
6.2 Nitrate Ion Trends 6-6
6.3 Organic Carbon Trends 6-10
6.4 Elemental Carbon Trends 6-14
6.5 Fine Dust Mass Trends 6-18
6.6 Gravimetric $PM_{2.5}$ Fine Mass Trends 6-22
6.7 PM_{10} Trends 6-26
6.8 Coarse Mass Trends 6-29
6.9 f_{abs} Trends 6-33
6.10 Discussion 6-36
REFERENCES 6-40
Chapter 7. Trends in IMPROVE Reconstructed Light Extinction Coefficients 7-1
7.1 Ammonium Sulfate Light Extinction Coefficient Trends 7-2

7.2 Ammonium Nitrate Light Extinction Coefficient Trends 7-5
7.3 Particulate Organic Matter Light Extinction Coefficient Trends 7-8
7.4 Elemental Carbon Light Extinction Coefficient Trends 7-12
7.5 Fine Dust Light Extinction Coefficient Trends 7-15
7.6 Coarse Mass Light Extinction Coefficient Trends 7-19
7.7 Aerosol Extinction Coefficient Trends 7-23
7.8 Total Extinction Coefficient Trends 7-26
7.9 Deciview Trends 7-29
7.10 Discussion 7-32
REFERENCES 7-37
Chapter 8. IMPROVE Bibilography 2010 to Present 8-1

LIST OF FIGURES

Figure S.2.1. Locations of IMPROVE sites for all discontinued and current sites. IMPROVE regions are indicated by shading and bold text. Urban IMPROVE sites are identified by stars. Blue circles indicate sites with data used in the analyses in this report. S-4

Figure S.2.2. Current and discontinued Chemical Speciation Network (CSN) sites (grey and orange) operated by the Environmental Protection Agency. Regions are shown as shaded areas and bold text. Sites included in the analyses in this report are shown as orange circles. S-5

Figure S.3.1. 2016–2019 $PM_{2.5}$ ammonium sulfate (AS) annual mean mass concentrations ($\mu g\ m^{-3}$) for (a) IMPROVE and (b) IMPROVE and CSN. S-7

Figure S.3.2. 2016–2019 $PM_{2.5}$ ammonium nitrate (AN) annual mean mass concentrations ($\mu g\ m^{-3}$) for (a) IMPROVE and (b) IMPROVE and CSN. S-8

Figure S.3.3. 2016–2019 $PM_{2.5}$ particulate organic matter (POM) annual mean mass concentrations ($\mu g\ m^{-3}$) for (a) IMPROVE and (b) IMPROVE and CSN. S-8

Figure S.3.4. 2016–2019 $PM_{2.5}$ elemental carbon (EC) annual mean mass concentrations ($\mu g\ m^{-3}$) for (a) IMPROVE and (b) IMPROVE and CSN. S-9

Figure S.3.5. 2016–2019 $PM_{2.5}$ fine dust (FD) annual mean mass concentrations ($\mu g\ m^{-3}$) for (a) IMPROVE and (b) IMPROVE and CSN. S-10

Figure S.3.6. 2016–2019 $PM_{2.5}$ sea salt (SS) annual mean mass concentrations ($\mu g\ m^{-3}$) for (a) IMPROVE and (b) IMPROVE and CSN. S-10

Figure S.3.7. 2016–2019 $PM_{2.5}$ gravimetric annual mean fine mass (FM) concentrations ($\mu g\ m^{-3}$) for (a) IMPROVE and (b) IMPROVE and CSN. S-11

Figure S.3.8. 2016–2019 annual mean gravimetric coarse mass ($CM = PM_{10} - PM_{2.5}$) ($\mu g\ m^{-3}$) for (a) IMPROVE and (b) IMPROVE and EPA. S-11

Figure S.4.1. IMPROVE 2016–2019 regional monthly mean $PM_{2.5}$ mass concentrations ($\mu g\ m^{-3}$) for the eastern United States. Letters on the x-axis correspond to month and "A" corresponds to annual mean. Shaded areas in the map correspond to regions that include the sites used in the analysis, shown as blue dots. S-14

Figure S.4.2. IMPROVE 2016–2019 regional monthly mean $PM_{2.5}$ mass concentrations ($\mu g\ m^{-3}$) for the northwestern United States. Letters on the x-axis correspond to month and "A" corresponds to annual mean. Shaded areas in the map correspond to regions that include the sites used in the analysis, shown as blue dots. S-15

Figure S.4.3. IMPROVE 2016–2019 regional monthly mean $PM_{2.5}$ mass concentrations ($\mu g\ m^{-3}$) for the southwestern United States. Letters on the x-axis correspond to month and "A" corresponds to annual mean. Shaded areas in the map correspond to regions that include the sites used in the analysis, shown as blue dots. S-16

Figure S.4.4. CSN 2016–2019 regional monthly mean $PM_{2.5}$ mass concentrations ($\mu g\ m^{-3}$) for the eastern United States. Letters on the x-axis correspond to month and "A" corresponds to annual mean. Shaded areas in the map correspond to regions that include the sites used in the analysis, shown as orange dots. S-17

Figure S.4.5. CSN 2016–2019 regional monthly mean $PM_{2.5}$ mass concentrations ($\mu g\ m^{-3}$) for the northwestern United States. Letters on the x-axis correspond to month and "A" corresponds

to annual mean. Shaded areas in the map correspond to regions that include the sites used in the analysis, shown as orange dots. S-18

Figure S.4.6. CSN 2016–2019 regional monthly mean $PM_{2.5}$ mass concentrations ($\mu g\ m^{-3}$) for the northwestern United States. Letters on the x-axis correspond to month and "A" corresponds to annual mean. Shaded areas in the map correspond to regions that include the sites used in the analysis, shown as orange dots. S-19

Figure S.5.1. 2016–2019 annual mean ambient total reconstructed light extinction coefficient (b_{ext_tot}) (Mm^{-1}) for (a) IMPROVE and (b) IMPROVE and CSN. Annual mean deciview (dv) for (c) IMPROVE and (d) IMPROVE and CSN. Wavelength corresponds to 550 nm. S-26

Figure S.5.2. IMPROVE 2016–2019 regional monthly mean speciated fractional contributions to ambient aerosol light extinction coefficients (b_{ext}) for the eastern United States. Letters on the x-axis correspond to the month and "A" corresponds to annual mean. Shaded areas in the map correspond to regions that include sites used in the analysis, shown as blue dots. Wavelength corresponds to 550 nm. S-27

Figure S.5.3. IMPROVE 2016–2019 regional monthly mean speciated fractional contributions to ambient aerosol light extinction coefficients (b_{ext}) for the northwestern United States. Letters on the x-axis correspond to the month and "A" corresponds to annual mean. Shaded areas in the map correspond to regions that include sites used in the analysis, shown as blue dots. Wavelength corresponds to 550 nm. S-28

Figure S.5.4. IMPROVE 2016–2019 regional monthly mean speciated fractional contributions to ambient aerosol light extinction coefficients (b_{ext}) for the southwestern United States. Letters on the x-axis correspond to the month and "A" corresponds to annual mean. Shaded areas in the map correspond to regions that include sites used in the analysis, shown as blue dots. Wavelength corresponds to 550 nm. S-29

Figure S.5.5. CSN 2016–2019 regional monthly mean speciated fractional contributions to ambient aerosol light extinction coefficients (b_{ext}) for the eastern United States. Letters on the x-axis correspond to the month and "A" corresponds to annual mean. Shaded areas in the map correspond to regions that include sites used in the analysis, shown as orange dots. Wavelength corresponds to 550 nm. S-30

Figure S.5.6. 2016–2019 regional monthly mean speciated fractional contributions to ambient aerosol light extinction coefficients (b_{ext}) for the northwestern United States. Letters on the x-axis correspond to the month and "A" corresponds to annual mean. Shaded areas in the map correspond to regions that include sites used in the analysis, shown as orange dots. Wavelength corresponds to 550 nm. S-31

Figure S.5.7. CSN 2016–2019 regional monthly mean speciated fractional contributions to ambient aerosol light extinction coefficients (b_{ext}) for the southwestern United States. Letters on the x-axis correspond to the month and "A" corresponds to annual mean. Shaded areas in the map correspond to regions that include sites used in the analysis, shown as orange dots. Wavelength corresponds to 550 nm. S-32

Figure S.6.1.1. Annual mean sulfate ion mass trends (% yr^{-1}) for short-term (2000–2019) periods. Filled triangles correspond to statistically significant trends ($p \leq 0.05$). S-39

Figure S.6.1.2. Short-term (2000–2019) regional seasonal mean sulfate ion trends (% yr^{-1}) for major U.S. regions for winter, spring, summer, fall, and annual means. Regions are arranged

from western to eastern United States (AK = Alaska, HI = Hawaii, NW = Northwest, CA = California, SW = Southwest, Cen = Central, MiS = Midsouth, NE = Northeast, SE = Southeast, VIIS = Virgin Islands, and US = all sites). Statistically significant trends ($p \leq 0.05$) are denoted with "*". S-40

Figure S.6.2.1. Annual mean nitrate ion mass trends (% yr^{-1}) for short-term (2000–2019) periods. Filled triangles correspond to statistically significant trends ($p \leq 0.05$). S-41

Figure S.6.2.2. Short-term (2000–2019) regional seasonal mean nitrate ion trends (% yr^{-1}) for major U.S. regions for winter, spring, summer, fall, and annual means. Regions are arranged from western to eastern United States (AK = Alaska, HI = Hawaii, NW = Northwest, CA = California, SW = Southwest, Cen = Central, MiS = Midsouth, NE = Northeast, SE = Southeast, VIIS = Virgin Islands, and US = all sites). Statistically significant trends ($p \leq 0.05$) are denoted with "*". S-41

Figure S.6.3.1. Annual mean organic carbon mass trends (% yr^{-1}) for short-term (2000–2019) periods. Filled triangles correspond to statistically significant trends ($p \leq 0.05$). S-42

Figure S.6.3.2. Short-term (2000–2019) regional seasonal mean organic carbon (OC) trends (% yr^{-1}) for major U.S. regions for winter, spring, summer, fall, and annual means. Regions are arranged from western to eastern United States (AK = Alaska, HI = Hawaii, NW = Northwest, CA = California, SW = Southwest, Cen = Central, MiS = Midsouth, NE = Northeast, SE = Southeast, VIIS = Virgin Islands, and US = all sites). Statistically significant trends ($p \leq 0.05$) are denoted with "*"..... S-43

Figure S.6.4.1. Annual mean elemental carbon mass trends (% yr^{-1}) for short-term (2000–2019) periods. Filled triangles correspond to statistically significant trends ($p \leq 0.05$). S-44

Figure S.6.4.2. Short-term (2000–2019) regional seasonal mean elemental carbon (EC) trends (% yr^{-1}) for major U.S. regions for winter, spring, summer, fall, and annual means. Regions are arranged from western to eastern United States (AK = Alaska, HI = Hawaii, NW = Northwest, CA = California, SW = Southwest, Cen = Central, MiS = Midsouth, NE = Northeast, SE = Southeast, VIIS = Virgin Islands, and US = all sites). Statistically significant trends ($p \leq 0.05$) are denoted with "*"..... S-44

Figure S.6.5.1. Annual mean fine dust (FD) mass trends (% yr^{-1}) for short-term (2000–2019) periods. Filled triangles correspond to statistically significant trends ($p \leq 0.05$). S-45

Figure S.6.5.2. Short-term (2000–2019) regional seasonal mean fine dust mass trends (% yr^{-1}) for major U.S. regions for winter, spring, summer, fall, and annual means. Regions are arranged from western to eastern United States (AK = Alaska, HI = Hawaii, NW = Northwest, CA = California, SW = Southwest, Cen = Central, MiS = Midsouth, NE = Northeast, SE = Southeast, VIIS = Virgin Islands, and US = all sites). Statistically significant trends ($p \leq 0.05$) are denoted with "*"..... S-46

Figure S.6.6.1. Annual mean $PM_{2.5}$ gravimetric fine mass (FM) trends (% yr^{-1}) for short-term (2000–2019) periods. Filled triangles correspond to statistically significant trends ($p \leq 0.05$). S-47

Figure S.6.6.2. Short-term (2000–2019) regional seasonal mean gravimetric $PM_{2.5}$ fine mass (FM) trends (% yr^{-1}) for major U.S. regions for winter, spring, summer, fall, and annual means. Regions are arranged from western to eastern United States (AK = Alaska, HI = Hawaii, NW = Northwest, CA = California, SW = Southwest, Cen = Central, MiS = Midsouth, NE = Northeast,

SE = Southeast, VIIS = Virgin Islands, and US = all sites). Statistically significant trends ($p \leq 0.05$) are denoted with "*"..... S-47

Figure S.6.7.1 Annual mean coarse mass (CM) trends (% yr^{-1}) for short-term (2000–2019) periods. Filled triangles correspond to statistically significant trends ($p \leq 0.05$)..... S-48

Figure S.6.7.2. Short-term (2000–2019) regional seasonal mean coarse mass (CM) trends (% yr^{-1}) for major U.S. regions for winter, spring, summer, fall, and annual means. Regions are arranged from western to eastern United States (AK = Alaska, HI = Hawaii, NW = Northwest, CA = California, SW = Southwest, Cen = Central, MiS = Midsouth, NE = Northeast, SE = Southeast, VIIS = Virgin Islands, and US = all sites). Statistically significant trends ($p \leq 0.05$) are denoted with "*"..... S-48

Figure S.6.8. Short-term (2001–2019) timelines of IMPROVE regional, annual mean mass concentrations (µg m^{-3}) for sulfate ion, nitrate ion, organic carbon (OC), elemental carbon (EC), an fine dust (FD)..... S-48

Figure 1.1. Class I areas of the United States. Shading identifies the managing agency of each CIA..... 1-3

Figure 1.2. Locations of IMPROVE sites for all discontinued and current sites. IMPROVE regions are indicated by shading and bold text. Urban IMPROVE sites are identified by stars. Blue circles indicate sites with data used in the analyses in this report..... 1-5

Figure 1.3. IMPROVE sampler showing the four modules with separate inlets and pumps. Substrates with analyses performed for each module are also shown..... 1-15

Figure 1.4. Version II IMPROVE sampler $PM_{2.5}$ module..... 1-16

Figure 1.5. IMPROVE XRF field blank concentrations (ng m^{-3}) for elemental species from January 2019 to January 2021..... 1-20

Figure 1.6. IMPROVE monthly median field blank concentrations (µg m^{-3}) for ions for 2016 through 2020..... 1-21

Figure 1.7. IMPROVE carbon fraction monthly median field blank concentrations (µg m^{-3}) from 2016 through 2020..... 1-23

Figure 1.8. Locations of nephelometers and web cameras..... 1-25

Figure 1.9. Fraction of IMPROVE network samples from January 2019 through June 2020 weighed on the MTL automated weighing system (Luna), the manual balance, or a mix of the two (e.g., pre-sampling mass from MTL automated weighing system and post-sampling mass from manual balance)..... 1-31

Figure 1.10. Timeline of elemental characterization methods used to analyze IMPROVE samples at UC Davis. PANalytical XRF is abbreviated "E5"..... 1-32

Figure 1.11. Scatterplots showing the agreement between XRF analytical instruments for elements routinely measured above 3 times the reported MDLs. Black dotted lines show the reported MDLs for each element and instrument while gray dashed lines show a 1:1 agreement, not a regression line. Data are for three sites (GRSM1, MORA1, and PORE1)..... 1-33

Figure 1.12. Time series of $PM_{2.5}$ (µg/filter) on Teflon filter field blanks (1 January 2011 through 30 June 2020). Blue vertical lines indicate manufacturer lot transition, where Pall

Corporation is the manufacturer. Red vertical line indicates manufacturer transition to Measurement Technology Laboratories (MTL) as manufacturer. 1-41

Figure 1.13. Time series of PM_{10} (µg/filter) on Teflon filter field blanks (1 January 2011 through 30 June 2020). Blue vertical lines indicate manufacturer lot transition, where Pall Corporation is the manufacturer. Red vertical line indicates manufacturer transition to Measurement Technology Laboratories (MTL) as manufacturer. 1-41

Figure 1.14. IMRPOVE field site audits from 2016–2022. Blue symbols correspond to audited sites; red symbols are sites yet to have a technical audit. 1-45

Figure 1.15. Current and discontinued Chemical Speciation Network (CSN) sites operated by the Environmental Protection Agency. Regions are shown as shaded areas and bold text. Sites included in the analyses in this report are shown as orange circles. 1-48

Figure 1.16. Comparisons of monthly mean 2016–2019 $PM_{2.5}$ aerosol mass concentration data (µg m^{-3}) for four collocated IMPROVE and CSN sites (see text) for (a) organic carbon (OC), (b) elemental carbon (EC), (c) ammonium sulfate (AS), (d) ammonium nitrate (AN), (e) fine dust, (f) sea salt (SS), (g) $PM_{2.5}$ gravimetric fine mass (FM), and (h) reconstructed fine mass (RCFM). 1-53

Figure 2.2.1a. IMPROVE 2016–2019 $PM_{2.5}$ ammonium sulfate (AS) annual mean mass concentrations (µg m^{-3}). 2-5

Figure 2.2.1b. IMPROVE and CSN 2016–2019 $PM_{2.5}$ ammonium sulfate (AS) annual mean mass concentrations (µg m^{-3}). 2-6

Figure 2.2.1c. IMPROVE 2016–2019 annual mean fraction contributions of ammonium sulfate (AS) to $PM_{2.5}$ reconstructed fine mass (RCFM). 2-6

Figure 2.2.1d. IMPROVE and CSN 2016–2019 annual mean fraction contributions of ammonium sulfate (AS) to $PM_{2.5}$ reconstructed fine mass (RCFM). 2-7

Figure 2.2.2a. IMPROVE 2016–2019 $PM_{2.5}$ ammonium nitrate (AN) annual mean mass concentrations (µg m^{-3}). 2-9

Figure 2.2.2b. IMPROVE and CSN 2016–2019 $PM_{2.5}$ ammonium nitrate (AN) annual mean mass concentrations (µg m^{-3}). 2-9

Figure 2.2.2c. IMPROVE 2016–2019 annual mean fraction contributions of ammonium nitrate (AN) to $PM_{2.5}$ reconstructed fine mass (RCFM). 2-10

Figure 2.2.2d. IMPROVE and CSN 2016–2019 annual mean fractions of ammonium nitrate (AN) to $PM_{2.5}$ reconstructed fine mass (RCFM). 2-10

Figure 2.2.3a. IMPROVE 2016–2019 $PM_{2.5}$ particulate organic matter (POM) annual mean mass concentrations (µg m^{-3}). 2-12

Figure 2.2.3b. IMPROVE and CSN 2016–2019 $PM_{2.5}$ particulate organic matter (POM) annual mean mass concentrations (µg m^{-3}). 2-12

Figure 2.2.3c. IMPROVE 2016–2019 annual mean fraction contributions of particulate organic matter (POM) to $PM_{2.5}$ reconstructed fine mass (RCFM). 2-13

Figure 2.2.3d. IMPROVE and CSN 2016–2019 annual mean fraction contributions of particulate organic matter (POM) to $PM_{2.5}$ reconstructed fine mass (RCFM). 2-13

Figure 2.2.4a. IMPROVE 2016–2019 $PM_{2.5}$ elemental carbon (EC) annual mean mass concentrations (μg m^{-3}). 2-15

Figure 2.2.4b. IMPROVE and CSN 2016–2019 $PM_{2.5}$ elemental carbon (EC) annual mean mass concentrations (μg m^{-3}). 2-15

Figure 2.2.4c. IMPROVE 2016–2019 annual mean fraction contributions of elemental carbon (EC) to $PM_{2.5}$ reconstructed fine mass (RCFM). 2-16

Figure 2.2.4d. IMPROVE and CSN 2016–2019 annual mean fraction contributions of elemental carbon (EC) to $PM_{2.5}$ reconstructed fine mass (RCFM). 2-16

Figure 2.2.5. IMPROVE 2016–2019 $PM_{2.5}$ annual mean filter absorption (f_{abs}) (Mm^{-1}). .. 2-17

Figure 2.2.6a. IMPROVE 2016–2019 $PM_{2.5}$ fine dust annual mean mass concentrations (μg m^{-3}). 2-19

Figure 2.2.6b. IMPROVE and CSN 2016–2019 $PM_{2.5}$ fine dust annual mean mass concentrations (μg m^{-3}). 2-20

Figure 2.2.6c. IMPROVE 2016–2019 annual mean fraction contributions of fine dust to $PM_{2.5}$ reconstructed fine mass (RCFM). 2-20

Figure 2.2.6d. IMPROVE and CSN 2016–2019 annual mean fraction contributions of fine dust to $PM_{2.5}$ reconstructed fine mass (RCFM). 2-21

Figure 2.2.7a. IMPROVE 2016–2019 $PM_{2.5}$ sea salt (SS) annual mean mass concentrations (μg m^{-3}). 2-22

Figure 2.2.7b. IMPROVE and CSN 2016–2019 $PM_{2.5}$ sea salt (SS) annual mean mass concentrations (μg m^{-3}). 2-23

Figure 2.2.7c. IMPROVE 2016–2019 annual mean fraction contributions of sea salt to $PM_{2.5}$ reconstructed fine mass (RCFM). 2-23

Figure 2.2.7d. IMPROVE and CSN 2016–2019 annual mean fraction contributions of sea salt (SS) to $PM_{2.5}$ reconstructed fine mass (RCFM). 2-24

Figure 2.2.8a. IMPROVE 2016–2019 $PM_{2.5}$ annual mean gravimetric fine mass (FM) concentrations (μg m^{-3}). 2-25

Figure 2.2.8b. IMPROVE and CSN 2016–2019 $PM_{2.5}$ annual mean gravimetric fine mass (FM) concentrations (μg m^{-3}). 2-25

Figure 2.2.9a. IMPROVE 2016–2019 $PM_{2.5}$ annual mean reconstructed fine mass (RCFM) concentrations (μg m^{-3}). 2-26

Figure 2.2.9b. IMPROVE and CSN 2016–2019 $PM_{2.5}$ annual mean reconstructed fine mass (RCFM) concentrations (μg m^{-3}). 2-27

Figure 2.2.10a. IMPROVE 2016–2019 annual mean $PM_{2.5}$ residuals (FM - RCFM) between $PM_{2.5}$ gravimetric fine mass (FM) and reconstructed fine mass (RCFM) (μg m^{-3}). 2-28

Figure 2.2.10b. IMPROVE and CSN 2016–2019 annual mean $PM_{2.5}$ residuals (FM - RCFM) between $PM_{2.5}$ gravimetric fine mass (FM) and reconstructed fine mass (RCFM) (μg m^{-3}). ... 2-28

Figure 2.2.11a. IMPROVE 2016–2019 annual mean PM_{10} mass (μg m^{-3}). 2-30

Figure 2.2.11b. IMPROVE and EPA 2016–2019 annual mean PM_{10} mass (μg m^{-3}). 2-30

Figure 2.2.12a. IMPROVE 2016–2019 annual mean coarse mass (CM = PM_{10} - $PM_{2.5}$) (μg m^{-3}). 2-31

Figure 2.2.12b. IMPROVE and EPA 2016–2019 annual mean coarse mass (CM = PM_{10} - $PM_{2.5}$) (μg m^{-3}). 2-32

Figure 2.2.12c. IMPROVE 2016–2019 annual mean fraction contributions of CM to PM_{10} gravimetric mass. 2-33

Figure 2.2.12d. IMPROVE and EPA 2016–2019 annual mean fraction contributions of CM to PM_{10} gravimetric mass. 2-33

Figure 3.1.1. IMPROVE 2016–2019 regional monthly mean $PM_{2.5}$ mass concentrations (μg m^{-3}) for the eastern United States. Letters on the x-axis correspond to month and "A" corresponds to annual mean. Shaded areas in the map correspond to regions that include the sites used in the analysis, shown as blue dots. 3-3

Figure 3.1.2. IMPROVE 2016–2019 regional monthly mean $PM_{2.5}$ mass concentrations (μg m^{-3}) for the northwestern United States. Letters on the x-axis correspond to month and "A" corresponds to annual mean. Shaded areas in the map correspond to regions that include the sites used in the analysis, shown as blue dots. 3-4

Figure 3.1.3. IMPROVE 2016–2019 regional monthly mean $PM_{2.5}$ mass concentrations (μg m^{-3}) for the southwestern United States. Letters on the x-axis correspond to month and "A" corresponds to annual mean. Shaded areas in the map correspond to regions that include the sites used in the analysis, shown as blue dots. 3-5

Figure 3.1.4. IMPROVE 2016–2019 regional monthly mean $PM_{2.5}$ reconstructed fine mass fractions for the eastern United States. Letters on the x-axis correspond to month and "A" corresponds to annual mean. Shaded areas in the map correspond to regions that include the sites used in the analysis, shown as blue dots. 3-6

Figure 3.1.5. IMPROVE 2016–2019 regional monthly mean $PM_{2.5}$ reconstructed fine mass fractions for the northwestern United States. Letters on the x-axis correspond to month and "A" corresponds to annual mean. Shaded areas in the map correspond to regions that include the sites used in the analysis, shown as blue dots. 3-7

Figure 3.1.6. IMPROVE 2016–2019 regional monthly mean $PM_{2.5}$ reconstructed fine mass fractions for the southwestern United States. Letters on the x-axis correspond to month and "A" corresponds to annual mean. Shaded areas in the map correspond to regions that include the sites used in the analysis, shown as blue dots. 3-8

Figure 3.1.7. CSN 2016–2019 regional monthly mean $PM_{2.5}$ mass concentrations (μg m^{-3}) for the eastern United States. Letters on the x-axis correspond to month and "A" corresponds to annual mean. Shaded areas in the map correspond to regions that include the sites used in the analysis, shown as orange dots. 3-9

Figure 3.1.8. CSN 2016–2019 regional monthly mean $PM_{2.5}$ mass concentrations (μg m^{-3}) for the northwestern United States. Letters on the x-axis correspond to month and "A" corresponds to annual mean. Shaded areas in the map correspond to regions that include the sites used in the analysis, shown as orange dots. 3-10

Figure 3.1.9. CSN 2016–2019 regional monthly mean $PM_{2.5}$ mass concentrations (μg m^{-3}) for the northwestern United States. Letters on the x-axis correspond to month and "A" corresponds

to annual mean. Shaded areas in the map correspond to regions that include the sites used in the analysis, shown as orange dots. 3-11

Figure 3.1.10. CSN 2016–2019 regional monthly mean $PM_{2.5}$ reconstructed fine mass fractions for the eastern United States. Letters on the x-axis correspond to month and "A" corresponds to annual mean. Shaded areas in the map correspond to regions that include the sites used in the analysis, shown as orange dots..... 3-12

Figure 3.1.11. CSN 2016–2019 regional monthly mean $PM_{2.5}$ reconstructed fine mass fractions for the northwestern United States. Letters on the x-axis correspond to month and "A" corresponds to annual mean. Shaded areas in the map correspond to regions that include the sites used in the analysis, shown as orange dots..... 3-13

Figure 3.1.12. CSN 2016–2019 regional monthly mean $PM_{2.5}$ reconstructed fine mass fractions for the southwestern United States. Letters on the x-axis correspond to the month and "A" corresponds to annual mean. Shaded areas in the map correspond to regions that include the sites used in the analysis, shown as orange dots. 3-14

Figure 3.8.1. IMPROVE 2016–2019 regional monthly mean coarse mass (CM) concentrations (μg m^{-3}) for the eastern United States. Letters on the x-axis correspond to the month and "A" corresponds to annual mean. Shaded areas in the map correspond to regions that include the sites used in the analysis, shown as blue dots..... 3-25

Figure 3.8.2. IMPROVE 2016–2019 regional monthly mean coarse mass (CM) concentrations (μg m^{-3}) for the northwestern United States. Letters on the x-axis correspond to the month and "A" corresponds to annual mean. Shaded areas in the map correspond to regions that include the sites used in the analysis, shown as orange dots. 3-26

Figure 3.8.3. IMPROVE 2016–2019 regional monthly mean coarse mass (CM) concentrations (μg m^{-3}) for the southwestern United States. Letters on the x-axis correspond to the month and "A" corresponds to annual mean. Shaded areas in the map correspond to regions that include the sites used in the analysis, shown as orange dots. 3-27

Figure 4.1. (a) Humidification factors (f(RH)) as a function of relative humidity (RH, %) for AS. A lognormal mass size distribution with a geometric mass mean diameter of 0.3 μm and a geometric standard deviation of 2.0 was assumed. (b) $f(RH)_{SS}$ for SS with an assumed lognormal mass size distribution with a geometric mass mean diameter of 2.5 μm and a geometric standard deviation of 2.0. A wavelength of 550 nm was used. 4-3

Figure 4.2. Comparisons of 2016–2019 monthly mean coarse mass concentrations (CM, μg m^{-3}) for four collocated IMPROVE (measured) and CSN (interpolated) sites. CSN CM concentrations were spatially interpolated from EPA Federal Reference Method (FRM) sites. 4-5

Figure 4.2.1a. IMPROVE 2016–2019 $PM_{2.5}$ reconstructed ambient annual mean light extinction coefficients for ammonium sulfate (b_{ext_AS}, Mm^{-1}). Wavelength corresponds to 550 nm..... 4-6

Figure 4.2.1b. IMPROVE and CSN 2016–2019 $PM_{2.5}$ reconstructed ambient annual mean light extinction coefficients for ammonium sulfate (b_{ext_AS}, Mm^{-1}). Wavelength corresponds to 550 nm..... 4-6

Figure 4.2.1c. IMPROVE 2016–2019 annual mean fraction contributions of ambient ammonium sulfate light extinction coefficient (b_{ext_AS}) to reconstructed aerosol b_{ext}. Wavelength corresponds to 550 nm. 4-7

Figure 4.2.1d. IMPROVE and CSN 2016–2019 annual mean fraction contributions of ambient ammonium sulfate light extinction coefficient (b_{ext_AS}) to reconstructed aerosol b_{ext}. Wavelength corresponds to 550 nm. 4-8

Figure 4.2.2a. IMPROVE 2016–2019 $PM_{2.5}$ reconstructed ambient annual mean light extinction coefficients for ammonium nitrate (b_{ext_AN}, Mm^{-1}). Wavelength corresponds to 550 nm. 4-9

Figure 4.2.2b. IMPROVE and CSN 2016–2019 $PM_{2.5}$ reconstructed ambient annual mean light extinction coefficients for ammonium nitrate (b_{ext_AN}, Mm^{-1}). Wavelength corresponds to 550 nm. 4-9

Figure 4.2.2c. IMPROVE 2016–2019 annual mean fraction contributions of ambient ammonium nitrate light extinction coefficient (b_{ext_AN}) to reconstructed aerosol b_{ext}. Wavelength corresponds to 550 nm. 4-10

Figure 4.2.2d. IMPROVE and CSN 2016–2019 annual mean fraction contributions of ambient ammonium nitrate light extinction coefficient (b_{ext_AN}) to reconstructed aerosol b_{ext}. Wavelength corresponds to 550 nm. 4-11

Figure 4.2.3a. IMPROVE 2016–2019 $PM_{2.5}$ reconstructed ambient annual mean light extinction coefficients for particulate organic matter (b_{ext_POM}, Mm^{-1}). Wavelength corresponds to 550 nm. 4-12

Figure 4.2.3b. IMPROVE and CSN 2016–2019 $PM_{2.5}$ reconstructed ambient annual mean light extinction coefficients for particulate organic matter (b_{ext_POM}, Mm^{-1}). Wavelength corresponds to 550 nm. 4-12

Figure 4.2.3c. IMPROVE 2016–2019 annual mean fraction contributions of particulate organic matter light extinction coefficient (b_{ext_POM}) to reconstructed aerosol b_{ext}. Wavelength corresponds to 550 nm. 4-13

Figure 4.2.3d. IMPROVE and CSN 2016–2019 annual mean fraction contributions of particulate organic matter light extinction coefficient (b_{ext_POM}) to reconstructed aerosol b_{ext}. Wavelength corresponds to 550 nm. 4-14

Figure 4.2.4a. IMPROVE 2016–2019 $PM_{2.5}$ reconstructed ambient annual mean light extinction coefficients for elemental carbon (b_{ext_EC}, Mm^{-1}). Wavelength corresponds to 550 nm. 4-15

Figure 4.2.4b. IMPROVE and CSN 2016–2019 $PM_{2.5}$ reconstructed ambient annual mean light extinction coefficients for elemental carbon (b_{ext_EC}, Mm^{-1}). Wavelength corresponds to 550 nm. 4-15

Figure 4.2.4c. IMPROVE 2016–2019 annual mean fraction contributions of elemental carbon light extinction coefficient (b_{ext_EC}) to reconstructed aerosol b_{ext}. Wavelength corresponds to 550 nm. 4-16

Figure 4.2.4d. IMPROVE and CSN 2016–2019 annual mean fraction contributions of elemental carbon light extinction coefficient (b_{ext_EC}) to reconstructed aerosol b_{ext}. Wavelength corresponds to 550 nm. 4-17

Figure 4.2.5a. IMPROVE 2016–2019 $PM_{2.5}$ reconstructed ambient annual mean light extinction coefficients for fine dust (b_{ext_FD}, Mm^{-1}). Wavelength corresponds to 550 nm. 4-18

Figure 4.2.5b. IMPROVE and CSN 2016–2019 $PM_{2.5}$ reconstructed ambient annual mean light extinction coefficients for fine dust (b_{ext_FD}, Mm^{-1}). Wavelength corresponds to 550 nm. 4-18

Figure 4.2.5c. IMPROVE 2016–2019 annual mean fraction contributions of fine dust light extinction coefficient (b_{ext_FD}) to reconstructed aerosol b_{ext}. Wavelength corresponds to 550 nm. 4-19

Figure 4.2.5d. IMPROVE and CSN 2016–2019 annual mean fraction contributions of fine dust light extinction coefficient (b_{ext_FD}) to reconstructed aerosol b_{ext}. Wavelength corresponds to 550 nm. 4-19

Figure 4.2.6a. IMPROVE 2016–2019 $PM_{2.5}$ reconstructed ambient annual mean light extinction coefficients for sea salt (b_{ext_SS}, Mm^{-1}). Wavelength corresponds to 550 nm. 4-20

Figure 4.2.6b. IMPROVE and CSN 2016–2019 $PM_{2.5}$ reconstructed ambient annual mean light extinction coefficients for sea salt (b_{ext_SS}, Mm^{-1}). Wavelength corresponds to 550 nm. 4-21

Figure 4.2.6c. IMPROVE 2016–2019 annual mean fraction contributions of sea salt light extinction coefficient (b_{ext_SS}) to reconstructed aerosol b_{ext}. Wavelength corresponds to 550 nm... 4-22

Figure 4.2.6d. IMPROVE and CSN 2016–2019 annual mean fraction contributions of sea salt light extinction coefficient (b_{ext_SS}) to reconstructed aerosol b_{ext}. Wavelength corresponds to 550 nm. 4-22

Figure 4.2.7a. IMPROVE 2016–2019 $PM_{2.5}$ reconstructed ambient annual mean light extinction coefficients for coarse mass (b_{ext_CM}, Mm^{-1}). Wavelength corresponds to 550 nm. 4-23

Figure 4.2.7b. IMPROVE and CSN 2016–2019 $PM_{2.5}$ reconstructed ambient annual mean light extinction coefficients for coarse mass (b_{ext_CM}, Mm^{-1}). Wavelength corresponds to 550 nm. 4-24

Figure 4.2.7c. IMPROVE 2016–2019 annual mean fraction contributions of coarse mass light extinction coefficient (b_{ext_CM}) to reconstructed aerosol b_{ext}. Wavelength corresponds to 550 nm.. 4-25

Figure 4.2.7d. IMPROVE and CSN 2016–2019 annual mean fraction contributions of coarse mass light extinction coefficient (b_{ext_CM}) to reconstructed aerosol b_{ext}. Wavelength corresponds to 550 nm. 4-25

Figure 4.2.8a. IMPROVE 2016–2019 reconstructed ambient annual mean aerosol light extinction coefficients (b_{ext_aer}, Mm^{-1}) (no Rayleigh scattering). Wavelength corresponds to 550 nm. 4-26

Figure 4.2.8b. IMPROVE and CSN 2016–2019 $PM_{2.5}$ reconstructed ambient annual mean aerosol light extinction coefficients (b_{ext_aer}, Mm^{-1}) (no Rayleigh scattering). Wavelength corresponds to 550 nm. 4-27

Figure 4.2.9a. IMPROVE 2016–2019 annual mean reconstructed ambient total light extinction coefficients (b_{ext_tot}, Mm^{-1}) (aerosol + Rayleigh). Wavelength corresponds to 550 nm. 4-27

Figure 4.2.9b. IMPROVE 2016–2019 annual mean reconstructed ambient total light extinction coefficients (b_{ext_tot}, Mm^{-1}) (aerosol + Rayleigh). Wavelength corresponds to 550 nm. 4-28

Figure 4.2.10a. IMPROVE 2016–2019 annual mean deciview (dv). Wavelength corresponds to 550 nm. 4-29

Figure 4.2.10b. IMPROVE and CSN 2016–2019 annual mean deciview (dv). Wavelength corresponds to 550 nm. 4-29

Figure 5.1.1. IMPROVE 2016–2019 regional monthly mean ambient reconstructed speciated aerosol light extinction coefficients (Mm^{-1}) for the eastern United States. Letters on the x-axis correspond to the month and "A" corresponds to annual mean. Shaded areas in the map correspond to regions that include sites used in the analysis, shown as blue dots. Wavelength corresponds to 550 nm. 5-2

Figure 5.1.2. IMPROVE 2016–2019 regional monthly mean ambient reconstructed speciated aerosol light extinction coefficients (Mm^{-1}) for the northwestern United States. Letters on the x-axis correspond to the month and "A" corresponds to annual mean. Shaded areas in the map correspond to regions that include sites used in the analysis, shown as blue dots. Wavelength corresponds to 550 nm. 5-3

Figure 5.1.3. IMPROVE 2016–2019 regional monthly mean ambient reconstructed speciated aerosol light extinction coefficients (Mm^{-1}) for the southwestern United States. Letters on the x-axis correspond to the month and "A" corresponds to annual mean. Shaded areas in the map correspond to regions that include sites used in the analysis, shown as blue dots. Wavelength corresponds to 550 nm. 5-4

Figure 5.1.4. IMPROVE 2016–2019 regional monthly mean speciated fractional contributions to ambient aerosol light extinction coefficients for the eastern United States. Letters on the x-axis correspond to the month and "A" corresponds to annual mean. Shaded areas in the map correspond to regions that include sites used in the analysis, shown as blue dots. Wavelength corresponds to 550 nm. 5-6

Figure 5.1.5. IMPROVE 2016–2019 regional monthly mean speciated fractional contributions to ambient aerosol light extinction coefficients for the northwestern United States. Letters on the x-axis correspond to the month and "A" corresponds to annual mean. Shaded areas in the map correspond to regions that include sites used in the analysis, shown as blue dots. Wavelength corresponds to 550 nm. 5-7

Figure 5.1.6. IMPROVE 2016–2019 regional monthly mean speciated fractional contributions to ambient aerosol light extinction coefficients for the southwestern United States. Letters on the x-axis correspond to the month and "A" corresponds to annual mean. Shaded areas in the map correspond to regions that include sites used in the analysis, shown as blue dots. Wavelength corresponds to 550 nm. 5-8

Figure 5.1.7. CSN 2016–2019 regional monthly mean ambient reconstructed speciated aerosol light extinction coefficients (Mm^{-1}) for the eastern United States. Letters on the x-axis correspond to the month and "A" corresponds to annual mean. Shaded areas in the map

correspond to regions that include sites used in the analysis, shown as orange dots. Wavelength corresponds to 550 nm. 5-9

Figure 5.1.8. CSN 2016–2019 regional monthly mean ambient reconstructed speciated aerosol light extinction coefficients (Mm^{-1}) for the northwestern United States. Letters on the x-axis correspond to the month and "A" corresponds to annual mean. Shaded areas in the map correspond to regions that include sites used in the analysis, shown as orange dots. Wavelength corresponds to 550 nm. 5-10

Figure 5.1.9. CSN 2016–2019 regional monthly mean ambient reconstructed speciated aerosol light extinction coefficients (Mm^{-1}) for the southwestern United States. Letters on the x-axis correspond to the month and "A" corresponds to annual mean. Shaded areas in the map correspond to regions that include sites used in the analysis, shown as orange dots. Wavelength corresponds to 550 nm. 5-11

Figure 5.1.10. CSN 2016–2019 regional monthly mean speciated fractional contributions to ambient aerosol light extinction coefficients for the eastern United States. Letters on the x-axis correspond to the month and "A" corresponds to annual mean. Shaded areas in the map correspond to regions that include sites used in the analysis, shown as orange dots. Wavelength corresponds to 550 nm. 5-12

Figure 5.1.11. 2016–2019 regional monthly mean speciated fractional contributions to ambient aerosol light extinction coefficients for the northwestern United States. Letters on the x-axis correspond to the month and "A" corresponds to annual mean. Shaded areas in the map correspond to regions that include sites used in the analysis, shown as orange dots. Wavelength corresponds to 550 nm. 5-13

Figure 5.1.12. CSN 2016–2019 regional monthly mean speciated fractional contributions to ambient aerosol light extinction coefficients for the southwestern United States. Letters on the x-axis correspond to the month and "A" corresponds to annual mean. Shaded areas in the map correspond to regions that include sites used in the analysis, shown as orange dots. Wavelength corresponds to 550 nm. 5-14

Figure 6.0. IMPROVE regions defined to summarize regional mean trends. 6-2

Figure 6.1.1. Annual mean sulfate ion mass trends (% yr^{-1}) for (a) long-term (1990–2019) and (b) short-term (2000–2019) periods. Filled triangles correspond to statistically significant trends ($p \leq 0.05$). 6-3

Figure 6.1.2. Short-term (2000–2019) regional seasonal mean sulfate ion trends (% yr^{-1}) for major U.S. regions for winter, spring, summer, fall, and annual means. Regions are arranged from western to eastern United States (AK = Alaska, HI = Hawaii, NW = Northwest, CA= California, SW = Southwest, Cen = Central, MiS = Midsouth, NE = Northeast, SE = Southeast, VIIS = Virgin Islands, and US = all sites). Statistically significant trends ($p \leq 0.05$) are denoted with "*". 6-3

Figure 6.1.3. IMPROVE long-term (1990–2019) trends (% yr^{-1}) in (a) 10^{th} percentile sulfate ion concentrations and (b) 90^{th} percentile concentrations. Filled triangles correspond to statistically significant trends ($p \leq 0.05$). 6-4

Figure 6.1.4. IMPROVE short-term (2000–2019) trends (% yr^{-1}) in (a) 10^{th} percentile sulfate ion concentrations and (b) 90^{th} percentile concentrations. Filled triangles correspond to statistically significant trends ($p \leq 0.05$). 6-5

Figure 6.1.5. Short-term (2000–2019) regional mean trends (% yr^{-1}) in 10^{th}, 50^{th}, and 90^{th} percentile sulfate ion concentrations. Regions are arranged from western to eastern United States (AK = Alaska, HI = Hawaii, NW = Northwest, CA= California, SW = Southwest, Cen = Central, MiS = Midsouth, NE = Northeast, SE = Southeast, VIIS = Virgin Islands, and US = all sites). Statistically significant trends ($p \leq 0.05$) are denoted with "*". 6-6

Figure 6.2.1. Annual mean nitrate ion mass trends (% yr^{-1}) for (a) long-term (1990–2019) and (b) short-term (2000–2019) periods. Filled triangles correspond to statistically significant trends ($p \leq 0.05$). 6-7

Figure 6.2.2. Short-term (2000–2019) regional seasonal mean nitrate ion trends (% yr^{-1}) for major U.S. regions for winter, spring, summer, fall, and annual means. Regions are arranged from western to eastern United States (AK = Alaska, HI = Hawaii, NW = Northwest, CA= California, SW = Southwest, Cen = Central, MiS = Midsouth, NE = Northeast, SE = Southeast, VIIS = Virgin Islands, and US = all sites). Statistically significant trends ($p \leq 0.05$) are denoted with "*". 6-8

Figure 6.2.3. IMPROVE long-term (1990–2019) trends (% yr^{-1}) in (a) 10^{th} percentile nitrate ion concentrations and (b) 90^{th} percentile concentrations. Filled triangles correspond to statistically significant trends ($p \leq 0.05$). 6-9

Figure 6.2.4. IMPROVE short-term (2000–2019) trends (% yr^{-1}) in (a) 10^{th} percentile nitrate ion concentrations and (b) 90^{th} percentile concentrations. Filled triangles correspond to statistically significant trends ($p \leq 0.05$). 6-9

Figure 6.2.5. Short-term (2000–2019) regional mean trends (% yr^{-1}) in 10^{th}, 50^{th}, and 90^{th} percentile nitrate ion concentrations. Regions are arranged from western to eastern United States (AK = Alaska, HI = Hawaii, NW = Northwest, CA= California, SW = Southwest, Cen = Central, MiS = Midsouth, NE = Northeast, SE = Southeast, VIIS = Virgin Islands, and US = all sites). Statistically significant trends ($p \leq 0.05$) are denoted with "*". 6-10

Figure 6.3.1. Annual mean organic carbon (OC) mass trends (% yr^{-1}) for (a) long-term (1990–2019) and (b) short-term (2000–2019) periods. Filled triangles correspond to statistically significant trends ($p \leq 0.05$). 6-11

Figure 6.3.2. Short-term (2000–2019) regional seasonal mean organic carbon (OC) trends (% yr^{-1}) for major U.S. regions for winter, spring, summer, fall, and annual means. Regions are arranged from western to eastern United States (AK = Alaska, HI = Hawaii, NW = Northwest, CA= California, SW = Southwest, Cen = Central, MiS = Midsouth, NE = Northeast, SE = Southeast, VIIS = Virgin Islands, and US = all sites). Statistically significant trends ($p \leq 0.05$) are denoted with "*". 6-12

Figure 6.3.3. IMPROVE long-term (1990–2020) trends (% yr^{-1}) in (a) 10^{th} percentile organic carbon (OC) concentrations and (b) 90^{th} percentile concentrations. Filled triangles correspond to statistically significant trends ($p \leq 0.05$). 6-13

Figure 6.3.4. IMPROVE short-term (2000–2019) trends (% yr^{-1}) in (a) 10^{th} percentile organic carbon (OC) concentrations and (b) 90^{th} percentile concentrations. Filled triangles correspond to statistically significant trends ($p \leq 0.05$). 6-13

Figure 6.3.5. Short-term (2000-2019) regional mean trends (% yr^{-1}) in 10^{th}, 50^{th}, and 90^{th} percentile organic carbon (OC) concentrations. Regions are arranged from western to eastern United States (AK = Alaska, HI = Hawaii, NW = Northwest, CA= California, SW = Southwest,

Cen = Central, MiS = Midsouth, NE = Northeast, SE = Southeast, VIIS = Virgin Islands, and US = all sites). Statistically significant trends (p≤0.05) are denoted with "*". 6-14

Figure 6.4.1. Annual mean elemental carbon (EC) mass trends (% yr^{-1}) for (a) long-term (1990–2019) and (b) short-term (2000–2019) periods. Filled triangles correspond to statistically significant trends ($p \leq 0.05$). 6-15

Figure 6.4.2. Short-term (2000–2019) regional seasonal mean elemental carbon (EC) trends (% yr^{-1}) for major U.S. regions for winter, spring, summer, fall, and annual means. Regions are arranged from western to eastern United States (AK = Alaska, HI = Hawaii, NW = Northwest, CA= California, SW = Southwest, Cen = Central, MiS = Midsouth, NE = Northeast, SE = Southeast, VIIS = Virgin Islands, and US = all sites). Statistically significant trends ($p \leq 0.05$) are denoted with "*". 6-16

Figure 6.4.3. IMPROVE long-term (1990–2019) trends (% yr^{-1}) in (a) 10^{th} percentile elemental carbon (EC) concentrations and (b) 90^{th} percentile concentrations. Filled triangles correspond to statistically significant trends ($p \leq 0.05$). 6-17

Figure 6.4.4. IMPROVE short-term (2000–2019) trends (% yr^{-1}) in (a) 10^{th} percentile elemental carbon (EC) concentrations and (b) 90^{th} percentile concentrations. Filled triangles correspond to statistically significant trends ($p \leq 0.05$). 6-17

Figure 6.4.5. Short-term (2000–2019) regional mean trends (% yr^{-1}) in 10^{th}, 50^{th}, and 90^{th} percentile elemental carbon (EC) percentile concentrations. Regions are arranged from western to eastern United States (AK = Alaska, HI = Hawaii, NW = Northwest, CA= California, SW = Southwest, Cen = Central, MiS = Midsouth, NE = Northeast, SE = Southeast, VIIS = Virgin Islands, and US = all sites). Statistically significant trends ($p \leq 0.05$) are denoted with "*".... 6-18

Figure 6.5.1 Annual mean fine dust mass trends (% yr^{-1}) for (a) long-term (1990–2019) and (b) short-term (2000–2019) periods. Filled triangles correspond to statistically significant trends ($p \leq 0.05$). 6-19

Figure 6.5.2. Short-term (2000–2019) regional seasonal mean fine dust mass trends (% yr^{-1}) for major U.S. regions for winter, spring, summer, fall, and annual means. Regions are arranged from western to eastern United States (AK = Alaska, HI = Hawaii, NW = Northwest, CA= California, SW = Southwest, Cen = Central, MiS = Midsouth, NE = Northeast, SE = Southeast, VIIS = Virgin Islands, and US = all sites). Statistically significant trends ($p \leq 0.05$) are denoted with "*". 6-20

Figure 6.5.3. IMPROVE long-term (1990–2019) trends (% yr^{-1}) in (a) 10^{th} percentile fine dust concentrations and (b) 90^{th} percentile concentrations. Filled triangles correspond to statistically significant trends ($p \leq 0.05$). 6-20

Figure 6.5.4. IMPROVE short-term (2000–2019) trends (% yr^{-1}) in (a) 10^{th} percentile fine dust concentrations and (b) 90^{th} percentile concentrations. Filled triangles correspond to statistically significant trends ($p \leq 0.05$). 6-21

Figure 6.5.5. Short-term (2000–2019) regional mean trends (% yr^{-1}) trends in 10^{th}, 50^{th}, and 90^{th} percentile fine dust concentrations. Regions are arranged from western to eastern United States (AK = Alaska, HI = Hawaii, NW = Northwest, CA= California, SW = Southwest, Cen = Central, MiS = Midsouth, NE = Northeast, SE = Southeast, VIIS = Virgin Islands, and US = all sites). Statistically significant trends ($p \leq 0.05$) are denoted with "*". 6-21

Figure 6.6.1. Annual mean gravimetric $PM_{2.5}$ fine mass (FM) trends (% yr^{-1}) for (a) long-term (1990–2019) and (b) short-term (2000–2019) periods. Filled triangles correspond to statistically significant trends ($p \leq 0.05$). 6-23

Figure 6.6.2. Short-term (2000–2019) regional seasonal mean gravimetric $PM_{2.5}$ fine mass (FM) trends (% yr^{-1}) for major U.S. regions for winter, spring, summer, fall, and annual means. Regions are arranged from western to eastern United States (AK = Alaska, HI = Hawaii, NW = Northwest, CA= California, SW = Southwest, Cen = Central, MiS = Midsouth, NE = Northeast, SE = Southeast, VIIS = Virgin Islands, and US = all sites). Statistically significant trends ($p \leq 0.05$) are denoted with "*"..... 6-23

Figure 6.6.3. IMPROVE long-term (1990–2019) trends (% yr^{-1}) in (a) 10^{th} percentile gravimetric $PM_{2.5}$ fine mass (FM) concentrations and (b) 90^{th} percentile concentrations. Filled triangles correspond to statistically significant trends ($p \leq 0.05$). 6-24

Figure 6.6.4. IMPROVE short-term (2000–2019) trends (% yr^{-1}) in (a) 10^{th} percentile gravimetric $PM_{2.5}$ fine mass (FM) concentrations and (b) 90^{th} percentile concentrations. Filled triangles correspond to statistically significant trends ($p \leq 0.05$). 6-25

Figure 6.6.5. Short-term (2000–2019) regional mean trends (% yr^{-1}) in 10^{th}, 50^{th}, and 90^{th} percentile gravimetric $PM_{2.5}$ fine mass (FM) concentrations. Regions are arranged from western to eastern United States (AK = Alaska, HI = Hawaii, NW = Northwest, CA= California, SW = Southwest, Cen = Central, MiS = Midsouth, NE = Northeast, SE = Southeast, VIIS = Virgin Islands, and US = all sites). Statistically significant trends ($p \leq 0.05$) are denoted with "*".... 6-25

Figure 6.7.1. Annual mean gravimetric PM_{10} mass trends (% yr^{-1}) for (a) long-term (1990–2019) and (b) short-term (2000–2019) periods. Filled triangles correspond to statistically significant trends ($p \leq 0.05$)..... 6-26

Figure 6.7.2. Short-term (2000–2019) regional seasonal mean gravimetric PM_{10} mass trends (% yr^{-1}) for major U.S. regions for winter, spring, summer, fall, and annual means. Regions are arranged from western to eastern United States (AK = Alaska, HI = Hawaii, NW = Northwest, CA= California, SW = Southwest, Cen = Central, MiS = Midsouth, NE = Northeast, SE = Southeast, VIIS = Virgin Islands, and US = all sites). Statistically significant trends ($p \leq 0.05$) are denoted with "*"..... 6-27

Figure 6.7.3. IMPROVE long-term (1990–2019) trends (% yr^{-1}) in (a) 10^{th} percentile gravimetric PM_{10} mass concentrations and (b) 90^{th} percentile concentrations. Filled triangles correspond to statistically significant trends ($p \leq 0.05$). 6-28

Figure 6.7.4. IMPROVE short-term (2000–2019) trends (% yr^{-1}) in (a) 10^{th} percentile gravimetric PM_{10} mass concentrations and (b) 90^{th} percentile concentrations. Filled triangles correspond to statistically significant trends ($p \leq 0.05$). 6-28

Figure 6.7.5. Short-term (2000–2019) regional mean trends (% yr^{-1}) in 10^{th}, 50^{th}, and 90^{th} percentile gravimetric PM_{10} mass concentrations. Regions are arranged from western to eastern United States (AK = Alaska, HI = Hawaii, NW = Northwest, CA= California, SW = Southwest, Cen = Central, MiS = Midsouth, NE = Northeast, SE = Southeast, VIIS = Virgin Islands, and US = all sites). Statistically significant trends ($p \leq 0.05$) are denoted with "*"..... 6-29

Figure 6.8.1. Annual mean coarse mass (CM) trends (% yr^{-1}) for (a) long-term (1990–2019) and (b) short-term (2000–2019) periods. Filled triangles correspond to statistically significant trends ($p \leq 0.05$)..... 6-30

Figure 6.8.2. Short-term (2000–2019) regional seasonal mean coarse mass (CM) trends (% yr^{-1}) for major U.S. regions for winter, spring, summer, fall, and annual means. Regions are arranged from western to eastern United States (AK = Alaska, HI = Hawaii, NW = Northwest, CA= California, SW = Southwest, Cen = Central, MiS = Midsouth, NE = Northeast, SE = Southeast, VIIS = Virgin Islands, and US = all sites). Statistically significant trends ($p \leq 0.05$) are denoted with "*"..... 6-31

Figure 6.8.3. IMPROVE long-term (1990–2019) trends (% yr^{-1}) in (a) 10^{th} percentile coarse mass (CM) concentrations and (b) 90^{th} percentile concentrations. Filled triangles correspond to statistically significant trends ($p \leq 0.05$). 6-32

Figure 6.8.4. IMPROVE short-term (2000–2019) trends (% yr^{-1}) in (a) 10^{th} percentile coarse mass (CM) concentrations and (b) 90^{th} percentile concentrations. Filled triangles correspond to statistically significant trends ($p \leq 0.05$). 6-33

Figure 6.8.5. Short-term (2000–2019) regional mean trends (% yr^{-1}) in 10^{th}, 50^{th}, and 90^{th} percentile coarse mass (CM) concentrations. Regions are arranged from western to eastern United States (AK = Alaska, HI = Hawaii, NW = Northwest, CA= California, SW = Southwest, Cen = Central, MiS = Midsouth, NE = Northeast, SE = Southeast, VIIS = Virgin Islands, and US = all sites). Statistically significant trends ($p \leq 0.05$) are denoted with "*"..... 6-33

Figure 6.9.1. Annual mean filter absorption (f_{abs}) short-term (2000–2019) trends (% yr^{-1}). Filled triangles correspond to statistically significant trends ($p \leq 0.05$). 6-34

Figure 6.9.2. Short-term (2000–2019) regional seasonal mean filter absorption (f_{abs}) trends (% yr^{-1}) for major U.S. regions for winter, spring, summer, fall, and annual means. Regions are arranged from western to eastern United States (AK = Alaska, HI = Hawaii, NW = Northwest, CA= California, SW = Southwest, Cen = Central, MiS = Midsouth, NE = Northeast, SE = Southeast, VIIS = Virgin Islands, and US = all sites). Statistically significant trends ($p \leq 0.05$) are denoted with "*"..... 6-35

Figure 6.9.3. IMPROVE short-term (2000–2019) trends (% yr^{-1}) in (a) 10^{th} percentile filter absorption (f_{abs}) and (b) 90^{th} percentile f_{abs}. Filled triangles correspond to statistically significant trends ($p \leq 0.05$). 6-36

Figure 6.9.4. Short-term (2000–2019) regional mean trends (% yr^{-1}) in 10^{th}, 50^{th}, and 90^{th} percentile filter absorption (f_{abs}). Regions are arranged from western to eastern United States (AK = Alaska, HI = Hawaii, NW = Northwest, CA= California, SW = Southwest, Cen = Central, MiS = Midsouth, NE = Northeast, SE = Southeast, VIIS = Virgin Islands, and US = all sites). Statistically significant trends ($p \leq 0.05$) are denoted with "*"..... 6-36

Figure 6.10.1. Short-term (2001–2019) timelines in IMPROVE regional, annual mean mass concentrations (µg m^{-3}) for sulfate ion, nitrate ion, organic carbon (OC), elemental carbon (EC), and fine dust (FD). 6-37

Figure 6.10.2. Short-term (2001–2019) timelines in IMPROVE regional, annual mean coarse mass (CM) concentrations (µg m^{-3}) 6-39

Figure 7.1.1. Annual mean ammonium sulfate b_{ext} (b_{ext_AS}) trends (% yr^{-1}) for (a) long-term (1990–2019) and (b) short-term (2000–2019) periods. Filled triangles correspond to statistically significant trends ($p \leq 0.05$)..... 7-2

Figure 7.1.2. Short-term (2000–2019) regional seasonal mean ammonium sulfate b_{ext} (b_{ext_AS}) trends (% yr^{-1}) for major U.S. regions for winter, spring, summer, fall, and annual means. Regions are arranged from western to eastern United States (AK = Alaska, HI = Hawaii, NW = Northwest, CA= California, SW = Southwest, Cen = Central, MiS = Midsouth, NE = Northeast, SE = Southeast, VIIS = Virgin Islands, and US = all sites). Statistically significant trends ($p \leq 0.05$) are denoted with "*". 7-3

Figure 7.1.3. IMPROVE long-term (1990–2019) trends (% yr^{-1}) in (a) 10^{th} percentile ammonium sulfate b_{ext} (b_{ext_AS}) and (b) 90^{th} percentile b_{ext_AS}. Filled triangles correspond to statistically significant trends ($p \leq 0.05$). 7-4

Figure 7.1.4. IMPROVE short-term (2000–2019) trends (% yr^{-1}) in (a) 10^{th} percentile ammonium sulfate b_{ext} (b_{ext_AS}) and (b) 90^{th} percentile b_{ext_AS}. Filled triangles correspond to statistically significant trends ($p \leq 0.05$). 7-4

Figure 7.1.5. Short-term (2000–2019) regional mean trends (% yr^{-1}) in 10^{th}, 50^{th}, and 90^{th} percentile ammonium sulfate b_{ext} (b_{ext_AS}). Regions are arranged from western to eastern United States (AK = Alaska, HI = Hawaii, NW = Northwest, CA= California, SW = Southwest, Cen = Central, MiS = Midsouth, NE = Northeast, SE = Southeast, VIIS = Virgin Islands, and US = all sites). Statistically significant trends ($p \leq 0.05$) are denoted with "*". 7-5

Figure 7.2.1. Annual mean ammonium nitrate b_{ext} (b_{ext_AN}) trends (% yr^{-1}) for (a) long-term (1990–2019) and (b) short-term (2000–2019) periods. Filled triangles correspond to statistically significant trends ($p \leq 0.05$). 7-6

Figure 7.2.2. Short-term (2000–2019) regional seasonal mean ammonium nitrate b_{ext} (b_{ext_AN}) trends (% yr^{-1}) for major U.S. regions for winter, spring, summer, fall, and annual means. Regions are arranged from western to eastern United States (AK = Alaska, HI = Hawaii, NW = Northwest, CA= California, SW = Southwest, Cen = Central, MiS = Midsouth, NE = Northeast, SE = Southeast, VIIS = Virgin Islands, and US = all sites). Statistically significant trends ($p \leq 0.05$) are denoted with "*". 7-6

Figure 7.2.3. IMPROVE long-term (1990–2019) trends (% yr^{-1}) in (a) 10^{th} percentile ammonium nitrate b_{ext} (b_{ext_AN}) and (b) 90^{th} percentile b_{ext_AN}. Filled triangles correspond to statistically significant trends ($p \leq 0.05$). 7-7

Figure 7.2.4. IMPROVE short-term (2000–2019) trends (% yr^{-1}) in (a) 10^{th} percentile ammonium nitrate b_{ext} (b_{ext_AN}) and (b) 90^{th} percentile b_{ext_AN}. Filled triangles correspond to statistically significant trends ($p \leq 0.05$). 7-8

Figure 7.2.5. Short-term (2000–2019) regional mean trends (% yr^{-1}) in 10^{th}, 50^{th}, and 90^{th} percentile ammonium nitrate b_{ext} (b_{ext_AN}). Regions are arranged from western to eastern United States (AK = Alaska, HI = Hawaii, NW = Northwest, CA= California, SW = Southwest, Cen = Central, MiS = Midsouth, NE = Northeast, SE = Southeast, VIIS = Virgin Islands, and US = all sites). Statistically significant trends ($p \leq 0.05$) are denoted with "*". 7-8

Figure 7.3.1. Annual mean particulate organic matter b_{ext} (b_{ext_POM}) trends (% yr^{-1}) for (a) long-term (1990–2019) and (b) short-term (2000–2019) periods. Filled triangles correspond to statistically significant trends ($p \leq 0.05$). 7-9

Figure 7.3.2. Short-term (2000-2019) regional, seasonal mean particulate organic matter b_{ext} (b_{ext_POM}) trends (% yr^{-1}) for major U.S. regions for winter, spring, summer, fall, and annual means. Regions are arranged from western to eastern United States (AK= Alaska, HI = Hawaii,

NW = Northwest, CA= California, SW = Southwest, Cen = Central, MiS = Midsouth, NE = Northeast, SE = Southeast, VIIS = Virgin Islands, and US = all sites). Statistically significant trends ($p \leq 0.05$) are denoted with "*". 7-10

Figure 7.3.3. IMPROVE long-term (1990–2019) trends (% yr^{-1}) in (a) 10^{th} percentile particulate organic matter b_{ext} (b_{ext_POM}) and (b) 90^{th} percentile b_{ext_POM}. Filled triangles correspond to statistically significant trends ($p \leq 0.05$). 7-11

Figure 7.3.4. IMPROVE long-term (1990–2019) trends (% yr^{-1}) in (a) 10^{th} percentile particulate organic matter b_{ext} (b_{ext_POM}) and (b) 90^{th} percentile b_{ext_POM}. Filled triangles correspond to statistically significant trends ($p \leq 0.05$). 7-11

Figure 7.3.5. Short-term (2000-2019) regional mean trends (% yr^{-1}) in 10^{th}, 50^{th}, and 90^{th} percentile particulate organic matter b_{ext} (b_{ext_POM}). Regions are arranged from western to eastern United States (AK = Alaska, HI = Hawaii, NW = Northwest, CA= California, SW = Southwest, Cen = Central, MiS = Midsouth, NE = Northeast, SE = Southeast, VIIS = Virgin Islands, and US = all sites). Statistically significant trends ($p \leq 0.05$) are denoted with "*". 7-12

Figure 7.4.1. Annual mean elemental carbon b_{ext} (b_{ext_EC}) trends for (a) long-term (1990–2019) and (b) short-term (2000–2019) periods. Filled triangles correspond to statistically significant trends ($p \leq 0.05$). 7-13

Figure 7.4.2. Short-term (2000–2019) regional seasonal mean elemental carbon b_{ext} (b_{ext_EC}) trends (% yr^{-1}) for major U.S. regions for winter, spring, summer, fall, and annual means. Regions are arranged from western to eastern United States (AK = Alaska, HI = Hawaii, NW = Northwest, CA= California, SW = Southwest, Cen = Central, MiS = Midsouth, NE = Northeast, SE = Southeast, VIIS = Virgin Islands, and US = all sites). Statistically significant trends ($p \leq 0.05$) are denoted with "*". 7-13

Figure 7.4.3. IMPROVE long-term (1990–2019) trends (% yr^{-1}) in (a) 10^{th} percentile elemental carbon b_{ext} (b_{ext_EC}) and (b) 90^{th} percentile b_{ext_EC}. Filled triangles correspond to statistically significant trends ($p \leq 0.05$). 7-14

Figure 7.4.4. IMPROVE short-term (2000–2019) trends (% yr^{-1}) in (a) 10^{th} percentile elemental carbon b_{ext} (b_{ext_EC}) and (b) 90^{th} percentile b_{ext_EC}. Filled triangles correspond to statistically significant trends ($p \leq 0.05$). 7-15

Figure 7.4.5. Short-term (2000–2019) regional mean trends (% yr^{-1}) in 10^{th}, 50^{th}, and 90^{th} percentile elemental carbon b_{ext} (b_{ext_EC}). Regions are arranged from western to eastern United States (AK = Alaska, HI = Hawaii, NW = Northwest, CA= California, SW = Southwest, Cen = Central, MiS = Midsouth, NE = Northeast, SE = Southeast, VIIS = Virgin Islands, and US = all sites). Statistically significant trends ($p \leq 0.05$) are denoted with "*". 7-15

Figure 7.5.1 Annual mean fine dust b_{ext} (b_{ext_FD}) trends (% yr^{-1}) for (a) long-term (1990–2019) and (b) short-term (2000–2019) periods. Filled triangles correspond to statistically significant trends ($p \leq 0.05$). 7-16

Figure 7.5.2. Short-term (2000-2019) regional seasonal mean fine dust b_{ext} (b_{ext_FD}) trends (% yr^{-1}) for major U.S. regions for winter, spring, summer, fall, and annual means. Regions are arranged from western to eastern United States (AK = Alaska, HI = Hawaii, NW = Northwest, CA= California, SW = Southwest, Cen = Central, MiS = Midsouth, NE = Northeast, SE = Southeast, VIIS = Virgin Islands, and US = all sites). Statistically significant trends ($p \leq 0.05$) are denoted with "*". 7-17

Figure 7.5.3. IMPROVE long-term (1990–2019) trends (% yr^{-1}) in (a) 10^{th} percentile fine dust b_{ext} (b_{ext_FD}) and (b) 90^{th} percentile b_{ext_FD}. Filled triangles correspond to statistically significant trends ($p \leq 0.05$). 7-17

Figure 7.5.4. IMPROVE short-term (2000–2019) trends (% yr^{-1}) in (a) 10^{th} percentile fine dust b_{ext} (b_{ext_FD}) and (b) 90^{th} percentile b_{ext_FD}. Filled triangles correspond to statistically significant trends ($p \leq 0.05$). 7-18

Figure 7.5.5. Short-term (2000–2019) regional mean trends (%yr^{-1}) in 10^{th}, 50^{th}, and 90^{th} percentile fine dust b_{ext} (b_{ext_FD}). Regions are arranged from western to eastern United States (AK = Alaska, HI = Hawaii, NW = Northwest, CA= California, SW = Southwest, Cen = Central, MiS = Midsouth, NE = Northeast, SE = Southeast, VIIS = Virgin Islands, and US = all sites). Statistically significant trends ($p \leq 0.05$) are denoted with "*". 7-19

Figure 7.6.1. Annual mean coarse mass b_{ext} (b_{ext_CM}) trends (% yr^{-1}) for (a) long-term (1990–2019) and (b) short-term (2000–2019) periods. Filled triangles correspond to statistically significant trends ($p \leq 0.05$). 7-19

Figure 7.6.2. Short-term (2000–2019) regional seasonal mean coarse mass b_{ext} (b_{ext_CM}) trends (% yr^{-1}) for major U.S. regions for winter, spring, summer, fall, and annual means. Regions are arranged from western to eastern United States (AK = Alaska, HI = Hawaii, NW = Northwest, CA= California, SW = Southwest, Cen = Central, MiS = Midsouth, NE = Northeast, SE = Southeast, VIIS = Virgin Islands, and US = all sites). Statistically significant trends ($p \leq 0.05$) are denoted with "*". 7-20

Figure 7.6.3. IMPROVE long-term (1990–2019) trends (% yr^{-1}) in (a) 10^{th} percentile coarse mass b_{ext} (b_{ext_CM}) and (b) 90^{th} percentile b_{ext_CM}. Filled triangles correspond to statistically significant trends ($p \leq 0.05$). 7-21

Figure 7.6.4. IMPROVE short-term (2000–2019) trends (%yr^{-1}) in (a) 10^{th} percentile coarse mass b_{ext} (b_{ext_CM}) and (b) 90^{th} percentile b_{ext_CM}. Filled triangles correspond to statistically significant trends ($p \leq 0.05$). 7-22

Figure 7.6.5. Short-term (2000–2019) regional mean trends (% yr^{-1}) in 10^{th}, 50^{th}, and 90^{th} percentile coarse mass b_{ext} (b_{ext_CM}). Regions are arranged from western to eastern United States (AK = Alaska, HI = Hawaii, NW = Northwest, CA= California, SW = Southwest, Cen = Central, MiS = Midsouth, NE = Northeast, SE = Southeast, VIIS = Virgin Islands, and US = all sites). Statistically significant trends ($p \leq 0.05$) are denoted with "*". 7-22

Figure 7.7.1 Annual mean aerosol b_{ext} (b_{ext_aer}) trends (% yr^{-1}) for (a) long-term (1990–2019) and (b) short-term (2000–2019) periods. Filled triangles correspond to statistically significant trends ($p \leq 0.05$). 7-23

Figure 7.7.2. Short-term (2000–2019) regional seasonal mean aerosol b_{ext} (b_{ext_aer}) trends (%yr^{-1}) for major U.S. regions for winter, spring, summer, fall, and annual means. Regions are arranged from western to eastern United States (AK = Alaska, HI = Hawaii, NW = Northwest, CA= California, SW = Southwest, Cen = Central, MiS = Midsouth, NE = Northeast, SE = Southeast, VIIS = Virgin Islands, and US = all sites). Statistically significant trends ($p \leq 0.05$) are denoted with "*". 7-24

Figure 7.7.3. IMPROVE long-term (1990–2019) trends (% yr^{-1}) in (a) 10^{th} percentile aerosol b_{ext} (b_{ext_aer}) and (b) 90^{th} percentile b_{ext_aer}. Filled triangles correspond to statistically significant trends ($p \leq 0.05$). 7-24

Figure 7.7.4. IMPROVE short-term (2000–2019) trends (% yr^{-1}) in (a) 10^{th} percentile aerosol b_{ext} (b_{ext_aer}) and (b) 90^{th} percentile b_{ext_aer}. Filled triangles correspond to statistically significant trends ($p \leq 0.05$). 7-25

Figure 7.7.5. Short-term (2000–2019) regional mean trends (% yr^{-1}) in 10^{th}, 50^{th}, and 90^{th} percentile aerosol b_{ext} (b_{ext_aer}). Regions are arranged from western to eastern United States (AK = Alaska, HI = Hawaii, NW = Northwest, CA= California, SW = Southwest, Cen = Central, MiS = Midsouth, NE = Northeast, SE = Southeast, VIIS = Virgin Islands, and US = all sites). Statistically significant trends ($p \leq 0.05$) are denoted with "*". 7-26

Figure 7.8.1. Annual mean total b_{ext} (b_{ext_tot}) trends (% yr^{-1}) for (a) long-term (1990–2019) and (b) short-term (2000–2019) periods. Filled triangles correspond to statistically significant trends ($p \leq 0.05$). 7-27

Figure 7.8.2. Short-term (2000–2019) regional seasonal mean total b_{ext} (b_{ext_tot}) trends (% yr^{-1}) for major U.S. regions for winter, spring, summer, fall, and annual means. Regions are arranged from western to eastern United States (AK = Alaska, HI = Hawaii, NW = Northwest, CA= California, SW = Southwest, Cen = Central, MiS = Midsouth, NE = Northeast, SE = Southeast, VIIS = Virgin Islands, and US = all sites). Statistically significant trends ($p \leq 0.05$) are denoted with "*". 7-27

Figure 7.8.3. IMPROVE long-term (1990–2019) trends (% yr^{-1}) in (a) 10^{th} percentile total b_{ext} (b_{ext_tot}) and (b) 90^{th} percentile b_{ext_tot}. Filled triangles correspond to statistically significant trends ($p \leq 0.05$). 7-28

Figure 7.8.4. IMPROVE short-term (2000–2019) trends (% yr^{-1}) in (a) 10^{th} percentile total b_{ext} (b_{ext_tot}) and (b) 90^{th} percentile b_{ext_tot}. Filled triangles correspond to statistically significant trends ($p \leq 0.05$). 7-28

Figure 7.8.5. Short-term (2000–2019) regional mean trends (% yr^{-1}) in 10^{th}, 50^{th}, and 90^{th} percentile total b_{ext} (b_{ext_tot}). Regions are arranged from western to eastern United States (AK = Alaska, HI = Hawaii, NW = Northwest, CA= California, SW = Southwest, Cen = Central, MiS = Midsouth, NE = Northeast, SE = Southeast, VIIS = Virgin Islands, and US = all sites). Statistically significant trends ($p \leq 0.05$) are denoted with "*". 7-29

Figure 7.9.1 Annual mean deciview (dv) trends (% yr^{-1}) for (a) long-term (1990–2019) and (b) short-term (2000–2019) periods. Filled triangles correspond to statistically significant trends ($p \leq 0.05$). 7-30

Figure 7.9.2. Short-term (2000–2019) regional seasonal mean deciview (dv) trends (% yr^{-1}) for major U.S. regions for winter, spring, summer, fall, and annual means. Regions are arranged from western to eastern United States (AK = Alaska, HI = Hawaii, NW = Northwest, CA= California, SW = Southwest, Cen = Central, MiS = Midsouth, NE = Northeast, SE = Southeast, VIIS = Virgin Islands, and US = all sites). Statistically significant trends ($p \leq 0.05$) are denoted with "*". 7-30

Figure 7.9.3. IMPROVE long-term (1990–2019) trends (% yr^{-1}) in (a) 10^{th} percentile deciview (dv) and (b) 90^{th} percentile dv. Filled triangles correspond to statistically significant trends ($p \leq 0.05$). 7-31

Figure 7.9.4. IMPROVE short-term (2000–2019) trends (% yr^{-1}) in (a) 10^{th} percentile deciview (dv) and (b) 90^{th} percentile dv. Filled triangles correspond to statistically significant trends ($p \leq 0.05$). 7-31

Figure 7.9.5. Short-term (2000–2019) trends (% yr^{-1}) trends in 10^{th}, 50^{th}, and 90^{th} percentile deciview (dv). Regions are arranged from western to eastern United States (AK = Alaska, HI = Hawaii, NW = Northwest, CA= California, SW = Southwest, Cen = Central, MiS = Midsouth, NE = Northeast, SE = Southeast, VIIS = Virgin Islands, and US = all sites). Statistically significant trends ($p \leq 0.05$) are denoted with "*". 7-32

Figure 7.10.1. Short-term (2001-2019) timelines in IMPROVE regional, annual mean ambient speciated bext (Mm^{-1}) for ammonium sulfate (b_{ext_AS}), ammonium nitrate (b_{ext_AN}), particulate organic matter (b_{ext_POM}), elemental carbon (b_{ext_EC}), fine dust (b_{ext_FD}), and coarse mass (b_{ext_CM}). Wavelength corresponds to 500 nm. 7-33

Figure 7.10.2. Split-image of visibility conditions in Great Smoky Mountains NP, Tennessee (GRSM1), for 90^{th} percentile total extinction levels in 1990 (left side) and 2019 (right side). 7-35

Figure 7.10.3. Split-image of visibility conditions in San Gorgonio WA, California (SAGO1), for 90^{th} percentile total extinction levels in 1990 (left side) and 2019 (right side).. 7-35

Figure 7.10.4. Split-image of visibility conditions in Yosemite NP, California (YOSE1), for 90^{th} percentile total extinction levels in 1990 (left side) and 2019 (right side). 7-36

LIST OF TABLES

Table S.2. Comparisons between monthly mean data at collocated IMPROVE and CSN sites from 2016 through 2019. Species include organic carbon (OC), elemental carbon (LAC), ammonium sulfate (AS), ammonium nitrate (AN), fine dust (FD), sea salt (SS), $PM_{2.5}$ gravimetric fine mass (FM), and $PM_{2.5}$ reconstructed fine mass (RCFM). Positive biases correspond to higher CSN concentrations. S-6

Table 1.1. Currently operating and discontinued IMPROVE particulate monitoring sites. Sites are grouped by region, as displayed in Figure 1.2. 1-6

Table 1.2. Class I areas and representative monitoring sites. 1-11

Table 1.3. Sites with a fifth collocated module. 1-18

Table 1.4. IMPROVE nephelometer network site locations. 1-26

Table 1.5 Web camera network site locations. 1-28

Table 1.6. Changes and updates made to the UC Davis HIPS system. 1-34

Table 1.7. Major networkwide changes in sampling, analysis, and data reporting affecting samples collected January 2011 and later. 1-43

Table 1.8. Chemical Speciation Network (CSN) site location, elevation, setting and region. 1-49

Table 1.9. Comparisons between monthly mean data at collocated IMPROVE and CSN sites from 2016 through 2019. Species include organic carbon (OC), elemental carbon (EC), ammonium sulfate (AS), ammonium nitrate (AN), fine dust (FD), sea salt (SS), $PM_{2.5}$ gravimetric fine mass (FM), and $PM_{2.5}$ reconstructed fine mass (RCFM). Positive biases correspond to higher CSN concentrations. 1-53

Table 2.1. Form of molecular species assumed in this report. Units in $\mu g\ m^{-3}$ unless otherwise noted. 2-2

Table 2.2. OM/OC ratios used to calculate POM and applied in the reconstructed mass algorithm for the CSN and IMPROVE networks. 2-3

Table 6.0. Regions and states (abbreviations) used for regional mean trends. Sites within listed states were included in the corresponding region. 6-1

LIST OF APPENDICES

Appendix 1.1. A New Cost-Effective Analytical Method for IMPROVE: Nondestructive Infrared Analysis of PTFE Filters to Measure Organic, Elemental, and Total Carbon, Inorganic Ions, Soil Elements, Organic Matter (OM), and Organic Functional Groups

Appendix 1.2. Documentation of Changes in Analytical Methods and Data Processing Due to the Chemical Speciation Network (CSN) Contractor Changes in 2015

Appendix 2.1. Monthly Varying Organic Carbon to Mass Ratio

Appendix 2.2. 2016–2019 IMPROVE and CSN Annual Mean Mass Concentrations

Appendix 2.3. 2016–2019 IMPROVE and CSN Annual Mean Mass Fraction

Appendix 3.1. 2016–2019 IMPROVE and CSN Regional, Monthly Mean Mass Concentration

Appendix 3.2. 2016–2019 IMPROVE and CSN Regional, Monthly Mean Mass Fraction

Appendix 4.1. 2016–2019 IMPROVE Monthly Humidification Factors (f(RH))

Appendix 4.2. 2016–2019 CSN Monthly Humidification Factors (f(RH))

Appendix 4.3. 2016–2019 IMPROVE and CSN Annual Mean Light Extinction Coefficients

Appendix 4.4. 2016–2019 IMPROVE and CSN Annual Mean Light Extinction Coefficients Fraction

Appendix 5.1. 2016–2019 IMPROVE and CSN Regional, Monthly Mean Reconstructed Light Extinction Coefficients

Appendix 5.2. 2016–2019 IMPROVE and CSN Regional, Monthly Mean Reconstructed Light Extinction Coefficient Fraction

Appendix 6.1. IMPROVE Annual Mean Mass Trends

Appendix 6.2. IMPROVE Short-Term (2000–2019) Mass Percentile Trends

Appendix 6.3. IMPROVE Long-Term (1990–2019) Mass Percentile Trends

Appendix 7.1. IMPROVE Annual Mean Light Extinction Coefficient Trends

Appendix 7.2. IMPROVE Short-Term (2000–2019) Light Extinction Coefficient Percentile Trends

Appendix 7.3. IMPROVE Long-Term (1990–2019) Light Extinction Coefficient Percentile Trends

Appendix 8. Regional Haze Rule Metrics